Chemical Synthesis of the Fluorescent, Cyclic Dinucleotides c^thGAMP

Simon Veth[+],[a] Adrian Fuchs[+],[a] Dilara Özdemir[+],[a] Clemens Dialer,[a] David Jan Drexler,[b] Fabian Knechtel,[a] Gregor Witte,[b] Karl-Peter Hopfner,[b] Thomas Carell,*[a] and Evelyn Ploetz*[a]

The cGAS-STING pathway is known for its role in sensing cytosolic DNA introduced by a viral infection, bacterial invasion or tumorigenesis. Free DNA is recognized by the cyclic GMP-AMP synthase (cGAS) catalyzing the production of 2',3'-cyclic guanosine monophosphate-adenosine monophosphate (2',3'-cGAMP) in mammals. This cyclic dinucleotide acts as a second messenger, activating the stimulator of interferon genes (STING) that finally triggers the transcription of interferon genes and inflammatory cytokines. Due to the therapeutic potential of this pathway, both the production and the detection of cGAMP via fluorescent moieties for assay development is of great importance. Here, we introduce the paralleled synthetic access to the intrinsically fluorescent, cyclic dinucleotides 2'3'-c^thGAMP and 3'3'-c^thGAMP based on phosphoramidite and phosphate chemistry, adaptable for large scale synthesis. We examine their binding properties to murine and human STING and confirm biological activity including interferon induction by 2'3'-c^thGAMP in THP-1 monocytes. Two-photon imaging revealed successful cellular uptake of 2'3'-c^thGAMP in THP-1 cells.

Introduction

The innate immune system of eukaryotes is one of the first defense lines against invading pathogens.[1] To detect pathogens, the discrimination of molecular patterns from "self" (host) and "nonself" (e.g., microorganisms) is a fundamental process and relies on an array of pattern recognition receptors (PRRs). These PRRs are cell surface or intracellular receptors that distinguish pathogen-associated molecular patterns (PAMPs) from endogenous host patterns.[2] In addition to PAMPs, some PRRs recognize damage-associated molecular patterns (DAMPs) such as host-derived signals of cellular stress.[3] During the last decade, a cyclic dinucleotide (CDN) 2',3'-cyclic guanosine mono-phosphate-adenosine monophosphate (2'3'-cGAMP, **1**) was identified to be crucially involved in transmitting innate immune system signaling (Figure 1a).[4]
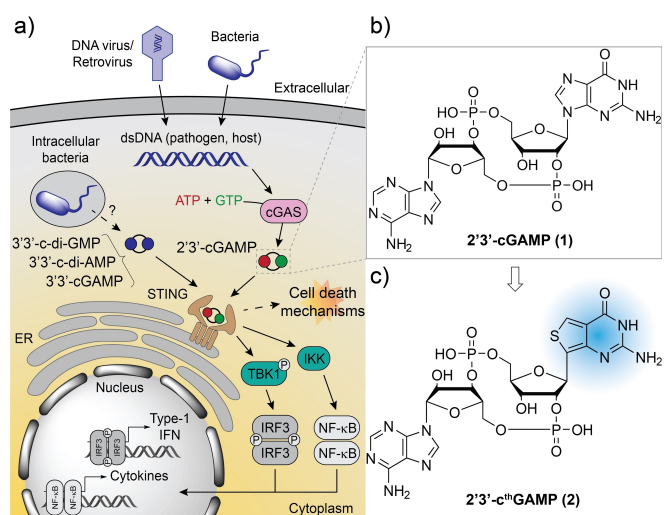

Figure 1. Biological role of CDNs. a) Molecular activation and regulation of the cGAS-cGAMP-STING pathway leading to interferon activation, inflammatory response and potential cell death. b) Structure of the CDN 2'3'-cGAMP. c) Chemical structure of the fluorescent analogue 2'3'-c^thGAMP (**2**).

[a] S. Veth,[+] A. Fuchs,[+] D. Özdemir,[+] Dr. C. Dialer, F. Knechtel, Prof. T. Carell, Dr. E. Ploetz
    Department of Chemistry and Center for NanoScience (CeNS)
    Ludwig-Maximilians-Universität München
    Butenandtstr. 5–13, 81377 Munich (Germany)
    E-mail: thomas.carell@cup.uni-muenchen.de
            evelyn.ploetz@cup.uni-muenchen.de
[b] Dr. D. J. Drexler, Dr. G. Witte, Prof. K.-P. Hopfner
    Gene Center and Department of Biochemistry
    Ludwig-Maximilians-Universität München
    Feodor-Lynen-Straße 25, 81377 Munich (Germany)
[+] These authors contributed equally to this work.

CDNs are found in vertebrates and prokaryotes alike and play an important role as second messengers.[5] While the CDNs from bacterial origin (e.g., 3'3'-c-di-GMP, 3'3'-c-di-AMP, 3'3'-cGAMP) are based on two canonical 3'-5' phosphodiester bonds,[6] the only CDN found in mammalian cells possesses a mixed 2'-5' and 3'-5' phosphodiester linkage (2'3'-cGAMP).[4]

2'3'-cGAMP plays a crucial role in the cyclic GMP-AMP synthase (cGAS)-stimulator of interferon genes (STING) pathway, which has emerged as a critical mechanism for coupling the sensing of double-stranded DNA (dsDNA) in the cytosol to the induction of innate immune defense programs. cGAS, an

ChemBioChem

Research Article
doi.org/10.1002/cbic.202200005

**Chemistry
Europe**
European Chemical
Societies Publishing

enzyme belonging to the family of DNA sensors, recognizes a broad repertoire of DNA species of both foreign (e.g., pathogens) and self-origin.[7] Upon binding to dsDNA in the cytosol, cGAS from bacteria are sensed by STING at the endoplasmic reticulum (ER),[8] triggering a signaling cascade by recruiting the kinases TBK1 and IKK, which results in the activation of interferon regulatory factor 3 (IRF3) and NF-κB.[9] IRF3 and NF-κB consecutively induce the expression of type-1 interferons (IFN), inflammatory cytokines and other interferon-stimulated genes (ISGs),[10] leading to a DNA-driven immune response. Depending on signaling strength, STING also results in the activation of other cellular processes such as apoptosis and necroptosis.[11]

The modification of CDNs with fluorescently active moieties holds great promises for the development of novel activity assays and emissive probes for following these key compounds *in vivo*, in order to deepen our fundamental understanding on the life cycle of CDNs, including biosynthesis, distribution, and degradation or recycling. For instance, a fluorescently labeled ATP analogue based on 2-aminopurine (2AP) was used in the cGAS-catalyzed formation of a fluorescent CDN (fGAMP) to characterize the length-dependency of cGAS activity.[12]

Depending on the desired application a drawback of many emissive nucleoside analogues, including the most prevalently used 2AP, could be their significant quenching upon incorporation into oligonucleotides and CDNs.[13] The group of Yitzhak Tor developed a highly emissive RNA alphabet (^{th}A, ^{th}G, ^{th}U, ^{th}C) with unparalleled structural isomorphicity to the native purine and pyrimidine bases derived from thieno[3,4-*d*]-pyrimidine as the heterocyclic nucleus. Besides excellent structural isomorphicity, good quantum yield ($\phi = 0.46$) and long excited-state lifetime (14.8 ns) were reported for ^{th}G in H_2O. Moreover, ^{th}G was found to show strong visible emission compared to 2AP even if "sandwiched" by two potential quenching guanosine residues in an oligonucleotide.[14]

In 2019, the enzymatic synthesis of a 2'3'-CDN bearing the ^{th}G base (2'3'-cthGAMP, **2**; Scheme 1) among 32 other CDNs was published focusing on the substrate specificity of cGAS derived from human, mouse and chicken as well as immunostimulatory properties in human peripheral blood mononuclear cells (PBMCs).[15] One year later, the enzymatic synthesis of ^{th}G-modified derivatives of bacterial 3'3'-c-di-GMP (3'3'-c-di-thGMP and 3'3'-c-thGGMP) were reported, highlighting their application in enzymatic assays and ability to induce a type-1 IFN response in THP-1 cells.[16] Cell experiments require large scales of the fluorescent, structural isomorph cGAMP mimics, which are hard to achieve by enzymatic pathways. To date, the organic synthesis of these compounds, as well as their application for cellular assays and fluorescent characterization *in vivo*, are missing.

Herein, we report the paralleled synthetic access to the cyclic dinucleotides 2'3'-cthGAMP and 3'3'-cthGAMP (Scheme 1) based on phosphoramidite and phosphate chemistry, suited for large scale synthesis. We highlight the differences in affinity of these CDNs to human and murine STING and focus on the scope and limitations of 2'3'-cthGAMP for *in vivo* studies in THP-1 cells using two-photon excitation microscopy.
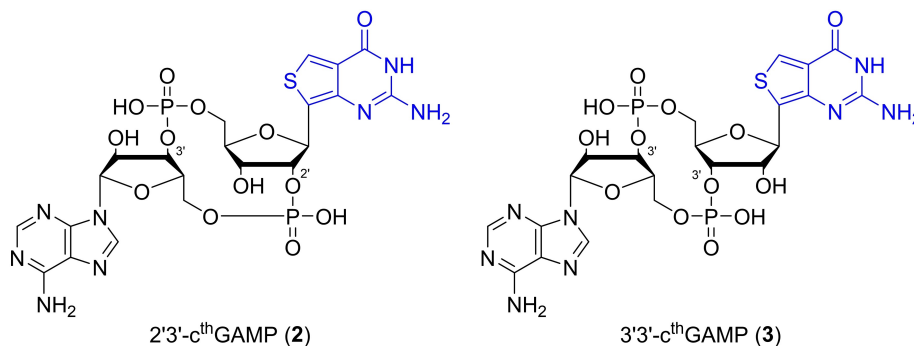
Results and Discussion

Synthesis

The paralleled synthesis of 2'3'-cthGAMP (**2**) and 3'3'-cthGAMP (**3**) is depicted in Scheme 1. Starting from the 5'-dimethoxytrityl (DMTr)- and dimethylformamidino (dmf)-protected ^{th}G nucleoside **4** (for synthetic details see Shin et al.),[14] TBS-protection did yield a regioisomeric mixture of the 3'-OTBS (**5**) and 2'-OTBS (**6**) protected nucleosides. Following a modified procedure from Ching et al.[17] these were converted to the corresponding phosphoramidites using commercially available 2-cyanoethyl *N,N,N',N'*-tetraisopropylphosphorodiamidite and pyridinium trifluoroacetate. The resulting 2'- and 3'-phosphoramidites were not isolated but instead the diisopropylamine functionality was directly displaced by allyl alcohol with the aid of 5-(benzylthio)-1*H*-tetrazole (BTT) activator followed by the *t*-BuOOH-mediated oxidation of the P(III)- to the P(V)-species and DMTr-deprotection in 3% dichloroacetic acid (DCA). In total, the four-step reaction sequence allowed to generate the allyl- and cyanoethyl-protected 2'-phosphate (**7**) and 3'-phosphate (**8**) in 56% yield. In a similar reaction sequence, commercially available DMT-2'-O-TBS-rA(Bz) phosphoramidite was then coupled to the free 5' OH groups of **7** and **8** with the aid of BTT activator, followed by oxidation and DMTr deprotection as described before. The resulting linear coupled dinucleotides were isolated in moderate yields, possessing the desired 2'3'- (**9**) and 3'3'- (**10**) connectivity. The deprotection of the allyl group with sodium iodide in refluxing acetone gave the alkoxides, which were cyclized using *N*-methylimidazole as nucleophilic catalyst, 2,4,6-triisopropylbenzenesulfonyl chloride (TPSCl) as condensing agent and molecular sieves (4 Å) as moisture scavenger to yield **11** and **12** in 49% yield over two steps. To minimize the formation of undesired side products by dimer formation, the cyclization reaction was carried out in dilute conditions (4 mM referred to starting material) to promote the intramolecular reaction. Treatment of **11** and **12** with a 1:1 mixture of ammonium hydroxide and methanol followed by triethylammonium fluoride resulted in the deprotection of the nucleobase protecting groups (dmf, Bz), β-cyanoethyl and silyl groups. After precipitation in cold acetone the resulting crude product was purified by reverse-phase HPLCs to separate and purify 2'3'-cthGAMP (**2**) and 3'3'-cthGAMP (**3**) in 13% yield for each CDN. The correct phosphodiester connectivity was NMR spectroscopically verified by ^{1}H-^{31}P-HMBC measurements (see Supporting Information).
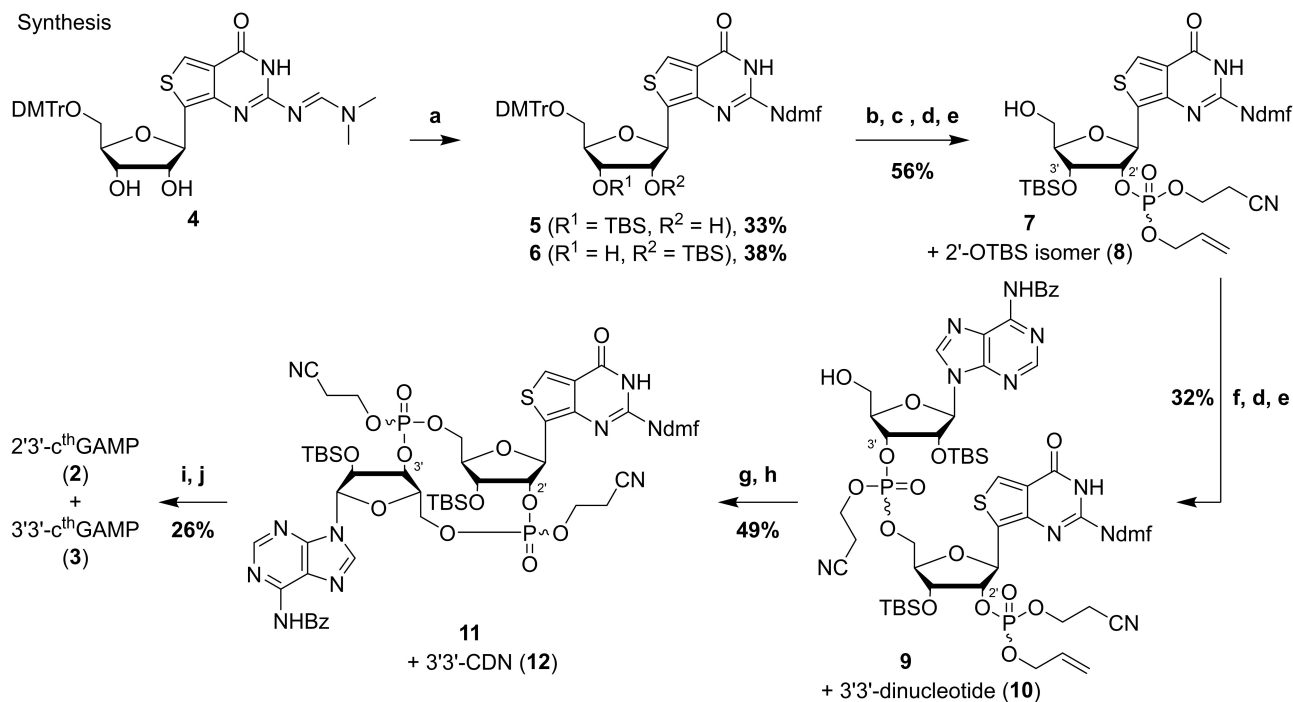
Biochemical characterization

With both target compounds in hands, we focused on evaluating their binding properties to murine and human STING. At first, we employed differential scanning fluorimetry (DSF) to determine the binding affinity of synthetic and natural CDNs to STING proteins by evaluating the difference in melting temperature of the STING protein with and without ligand (Supporting Figure S5.1). While 2'3'-cthGAMP shows reduced

ChemBioChem

Research Article
doi.org/10.1002/cbic.202200005

**Chemistry
Europe**
European Chemical
Societies Publishing

Products

2'3'-cthGAMP (**2**)

3'3'-cthGAMP (**3**)

Synthesis

Scheme 1. Paralleled synthesis of 2'3'-cthGAMP and 3'3'-cthGAMP. Products 2'3'-cthGAMP (**2**) and 3'3'-cthGAMP (**3**) and synthetic overview. a) TBSCl, imidazole, pyridine; b) 2-cyanoethyl *N,N,N',N'*-tetraisopropylphosphorodiamidite, pyridinium trifluoroacetate, MeCN; c) BTT, allyl alcohol; d) *t*-BuOOH, then NaHSO$_3$; e) 3% DCA in DCM; f) DMT-2'-O-TBS-rA(Bz) phosphoramidite, BTT, MeCN; g) NaI, acetone; h) TPSCl, N–Me-imidazole, THF; i) NH$_4$OH, MeOH; j) NEt$_3$·3HF, THF, then HPLC.

binding-affinity compared to natural 2'3'-cGAMP, the thermal shift assays revealed, that 3'3'-cthGAMP (**3**) does not possess favorable binding affinity to neither murine nor human STING. As a consequence, we focused on the characterization and application of 2'3'-cthGAMP (**2**) in the later part of this publication.

Using isothermal titration calorimetry (ITC; Figure 2), we found that 2'3'-cthGAMP (**2**) is a less potent binder than natural 2'3'-cGAMP ($k_D = \sim 4$ nM).[18] It shows a 120- and 4000-fold reduced affinity to murine STING (mSTING; $k_D = 455$ nm) and human STING (hSTING; $k_D = 15$ µm). The thermodynamic parameters highlight, that the binding of 2'3'-cthGAMP to both receptors is exergonic ($\Delta G_{mSTING} = -36.3$ kJ/mol, $\Delta G_{hSTING} = -27.9$ kJ/mol), however with opposite trend for enthalpy and entropy: binding to mSTING is favorable in terms of entropy ($-T\Delta S_{mSTING} = -59.3$ kJ/mol) and endothermic ($\Delta H_{mSTING} = 23.4$ kJ/mol). In contrast, binding to hSTING was found to be
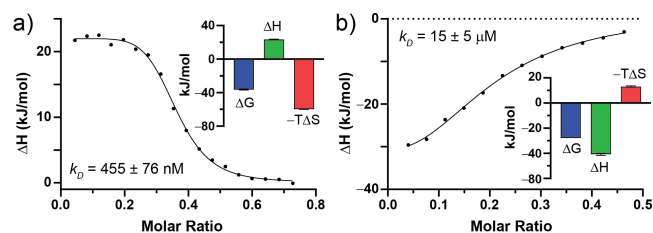

Figure 2. Binding to STING as measured by ITC. ITC curves and thermodynamic parameters for 2'3'-cthGAMP (**2**) bound to a) murine STING and b) human STING.

exothermic ($\Delta H_{hSTING} = -40.8$ kJ/mol) but entropically unfavorable ($-T\Delta S_{hSTING} = 13.1$ kJ/mol). Unlike the endothermic binding process of natural 2'3'-cGAMP to hSTING,[18] the data suggests that binding of 2'3'-cthGAMP might not trigger a full conforma-

ChemBioChem

Research Article
doi.org/10.1002/cbic.202200005

Chemistry
Europe
European Chemical
Societies Publishing

tional change in STING and, hence, a stabilized enclosure of the ligand. This observation would be in line with the reduced affinity of the synthetic compound.

Despite its reduced affinity, we set out next to investigate, whether binding of 2'3'-c[th]GAMP still activates STING signaling and consecutively interferon production. For this, we monitored the expression of the reporter gene Lucia luciferase in THP-1 Dual[TM] wild type (THP-1 monocytes) cells, which is under the control of the ISG54 promoter in conjunction with five IRF-stimulated response elements. Secretion of luciferase and hence activation of the IFN pathway was quantified by monitoring its luminescence in response to 2'3'-cGAMP and 2'3'-c[th]GAMP after transfection. 2'3'-c[th]GAMP showed a ~5-fold reduced but significant IRF activation compared to the natural compound (Supporting Information Figure S2).

Uptake in THP-1 cells

Having verified the biological potency of 2'3'-c[th]GAMP, we continued with THP-1 monocyte cells and monitored the uptake and effect on immune cells by following the fluorescent signature of the synthetic molecule *in vivo*. As reported, the 2'3'-c[th]GAMP features a broad absorption in the UV below 360 nm with a maximum around 315 nm (Figure 3a). Being excited at 310 nm, a blue photoluminescence was observed. The emission spectrum has a width of more than 200 nm, starting around 380 nm upwards with an emission maximum around 470 nm (Figure 3a). Since excitation sources in the UV and blue spectral range cause high background when being used for imaging cells due to scattering and autofluorescence, we employed two-photon imaging[19] using a pulsed laser excitation at 774 nm (Supporting Information Figure S5.3a–b). The fluorescence emission of 2'3'-c[th]GAMP (2) in water between 400–650 nm clearly showed a quadratic dependence on the exciting laser power (Supporting Information Figure S5.3c) confirming the nonlinear nature of the two-photon excitation.

Figure 3b (upper panels) shows the emitted autofluorescence of two THP-1 Dual[TM] cell lines, wild type (wt) and STING knock-out (STING KO), after two-photon excitation in the spectral range between 417 and 477 nm. Upon the addition of 2'3'-c[th]GAMP (2) to THP-1 wt cells, we expected an increase in overall brightness due to the intrinsic fluorescence of the compound. Instead, we observed a significant change in cell morphology combined with a strong decrease in emission (Figure 3c, upper panel, N = 91/129). In contrast, THP-1 STING-KO cells (Figure 3b, lower panel), which do not enter the consecutive immune response cascade, showed no morphological changes but only a slight swelling of the cell volume. Here, a significant increase in fluorescence intensity after 2'3'-c[th]GAMP uptake was monitored (Figure 3c, lower panel, N = 85/72). Both observations suggest, that 2'3'-c[th]GAMP is successfully taken up by both cell lines, however with different biological response: while cellular accumulation of 2'3'-c[th]GAMP leads to the expected brightness increase in THP-1 STING KO cells due to unavailability of the STING receptor and hence missing cellular response, the uptake in THP-1 wt cells triggered downstream
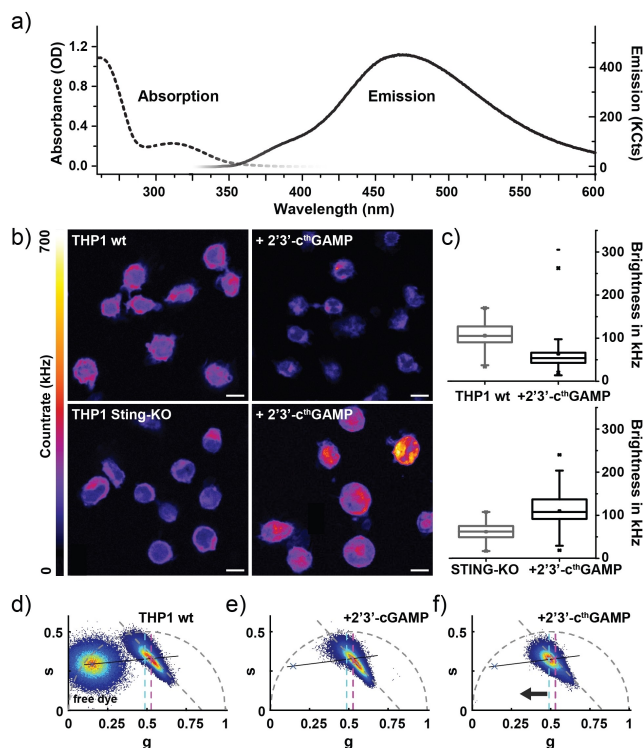

Figure 3. Fluorescence microscopy probing the cellular uptake of 2'3'-c[th]GAMP in THP-1 cells. a) Absorption (dotted line) and emission spectrum (solid line) of 52 μM 2'3'-c[th]GAMP in water after excitation at 310 nm. b-c) Two-photon images (b) and average cell brightness (c) of THP-1 wt cells (upper panel) and THP-1 STING-KO cells (lower panel) in absence and presence of 2'3'-c[th]GAMP. 2'3'-c[th]GAMP is biologically active in THP-1 wt cells leading to morphological changes and brightness decrease. In contrast, uptake of 2'3'-c[th]GAMP in STING knockout cells leads to a fluorescence increase. The emission was recorded between 417–477 nm and evaluated on average for 70–130 cells per condition. d–f) Phasor analysis of the average lifetime observed for THP-1 wt cells before (d) and after uptake of 50 μM 2'3'-cGAMP (e) and 200 μM 2'3'-c[th]GAMP (f). d) Phasor representation of the fluorescence signature of THP-1 wt cells and free 2'3'-c[th]GAMP in cell medium. The angled dotted line (grey) marks the multicomponent autofluorescent background in THP-1 wt cells. The center positions of the populations before (pink) and after (cyan) addition of 2'3'-c[th]GAMP (f) is marked with dotted lines. e) The addition of the non-fluorescent compound cGAMP triggers a shift in cellular autofluorescence towards shorter lifetimes and reduced brightness. f) The addition of 2'3'-c[th]GAMP leads to an off-axis shift towards free 2'3'-c[th]GAMP (along the black line), confirming the successful uptake.

processes due to activity of 2'3'-c[th]GAMP. Consecutive changes in cellular environment could affect the autofluorescent background, but also alter the photochemistry of the environmentally sensitive 2'3'-c[th]GAMP compound (see Supporting Information Figure S5.4.) by cellular interactions, leading to a decrease in fluorescence (if we anticipate the short time-window for free 2'3'-c[th]GAMP diffusion before binding to STING).

The autofluorescence signature of THP-1 overlaps with the emission spectrum of 2'3'-c[th]GAMP (2). To investigate whether the fluorescence increase observed for THP-1 STING KO cells can be directly linked to the uptake of 2'3'-c[th]GAMP (2), we evaluated the time-correlated single photon counting (TCSPC) data available for each image pixel in addition to the recorded

ChemBioChem

Research Article
doi.org/10.1002/cbic.202200005

**Chemistry
Europe**
European Chemical
Societies Publishing

brightness information. At first, we recorded two-photon images of free dye only in solution for comparison and calibration (Supporting Information Figure S5.4a-b). By analyzing the exponential decay of the TCSPC histograms, we found an approximately mono-exponential behavior (on long time-scales) of 16.8 ns for 2'3'-c[th]GAMP in water, similar to [th]G in water (14.8 ns).[14] In buffers, however, we observed a shortened lifetime of 6.2 ns in PBS and even 4.3 ns in THP-1 cell medium (Supporting Information Figure S5.4a). Due to this complex behavior and the multi-exponential nature of cellular autofluorescence, we expanded the lifetime evaluation using the phasor approach[20], which graphically translates the fluorescence lifetime decay into Fourier space (see Supporting Information Note 4.4 for details). This technique enables the detection of small contributions to a multi-component lifetime mixture.[20a] Here, mono-exponential decays will be observed on an arc of radius 0.5 with long lifetime components near the origin (0,0), while short lifetimes are expected to contribute near (1,0). On the other side, multi-exponential decay pathways or fluorescence decays of mixed species are expected inside the circle. They are composed of weighted linear compositions of the contributing mono-exponential species along the arc and obtained by vectorial addition of the weighted contributions by each fluorescence species (Supporting Information Figure S4.2d–f).

When analyzing the TCSPC data by the phasor approach, 2'3'-c[th]GAMP in PBS and cell medium is characterized by a bi-exponential, long-lived lifetime lying close to the left half-circle (Supporting Information Figure S5.4b), compared to the single-exponential signature of Atto532 in PBS on the circle. For the uptake of the fluorescent 2'3'-c[th]GAMP into THP-1 cells, we expect a mix between the signature of the fluorescent analogue and the autofluorescence of the cell line. The uptake should be seen by a shift of the cellular autofluorescence signature towards the population of the free dye, while for the natural, non-fluorescent 2'3'-cGAMP no change should occur.

THP-1 wt cells show a short-lived, multi-exponential autofluorescence of about 1.85 ns. Their population lies in the right half-circle compared to the longer-lived signature of the free 2'3'-c[th]GAMP in cell medium (Figure 3d). The addition of the natural analog 2'3'-cGAMP to THP-1 cells triggers a change in morphology and autofluorescent background. This change is evident by a shift along the grey dotted line towards shorter lifetimes and concomitantly reduced brightness. Besides a decrease of the average lifetime from 1.85 to 1.75 ns (Figure 3e), no shift towards the free 2'3'-c[th]GAMP compound (along the black line) was observed. Upon addition of 2'3'-c[th]GAMP, however, a clear shift towards the free fluorescent analog is observed (Figure 3f), as marked for the center position of cellular autofluorescent in absence (pink) and presence of 2'3'-c[th]GAMP (cyan). The cellular uptake of 2'3'-c[th]GAMP leads to an increase in average lifetime (2.05 ns) although a simultaneous reduction in autofluorescence background and lifetime is observed. For the STING KO line an identical behavior was detected (Supporting Information Figure 5.4c). Both findings, the brightness increase (Figure 3c, lower panel) as well as the lifetime shift towards the pure compound (Figure 3f) give clear

evidence, that 2'3'-c[th]GAMP was taken up into THP-1 monocytes.

Conclusion

In summary, we report the first organic synthesis of 2'3'-c[th]GAMP (**2**) and 3'3'-c[th]GAMP (**3**), which feature the fluorescent [th]G base. The described synthetic strategy - involving phosphoramidite and phosphate chemistry - provides direct access to large quantities of both immunostimulants and enabled us to carry out cell feeding experiments with 2'3'-c[th]GAMP (**2**) as well as subsequent two-photon microscopy on THP-1 cells. While biochemical as well as cell-based assays confirmed the biologically activity of the synthetically derived compound, we further verified its presence in cells using fluorescence imaging and lifetime. Moreover, our observations show that the fluorescence lifetime of 2'3'-c[th]GAMP (**2**) is highly dependent on its environment suggesting a complex photochemistry for CDNs in general including the synthesized compound. While suitable for two-photon excitation microscopy, the cellular application of the fluorescent 2'3'-cGAMP analogue including intracellular tracking and downstream monitoring is strongly dependent on the autofluorescence of the chosen cell line, which creates an additional cell dependent detection limit. The decreased binding affinity of 2'3'-c[th]GAMP (**2**) to human STING in combination with high EC50 values[15] indicate substantial shortcomings which need to be addressed in the future. Nevertheless, as second messengers with diverse roles in both prokaryotes and eukaryotes, both fluorescent c[th]GAMP analogues may well serve for enzymatic assays/screening assays for inhibitors of CDN metabolism enzymes facilitating the development of therapeutics that target the cGAS-STING signaling pathway.

Experimental Section

Detailed experimental procedures during the synthesis and characterization of the fluorescent dinucleotides, protein purification of murine and human STING receptors, cell culturing, and advanced fluorescence microscopy are provided in the Supporting Information.

Conflict of Interest

The authors declare no conflict of interest.

Data Availability Statement

The data that support the findings of this study are available from the corresponding author upon reasonable request.

[1] R. Medzhitov, C. A. Janeway, Jr., *Cell* **1997**, *91*, 295–298.
[2] S. Gordon, *Cell* **2002**, *111*, 927–930.
[3] K. Schroder, J. Tschopp, *Cell* **2010**, *140*, 821–832.
[4] A. Ablasser, M. Goldeck, T. Cavlar, T. Deimling, G. Witte, I. Röhl, K.-P. Hopfner, J. Ludwig, V. Hornung, *Nature* **2013**, *498*, 380–384.
[5] a) O. Danilchanka, J. J. Mekalanos, *Cell* **2013**, *154*, 962–970; b) L. Sun, J. Wu, F. Du, X. Chen, Z. Chen, *Science* **2013**, *339*, 786–791; c) U. Römling, M. Y. Galperin, M. Gomelsky, *Microbiol. Mol. Biol. Rev.* **2013**, *77*, 1–52.
[6] a) R. M. Corrigan, J. C. Abbott, H. Burhenne, V. Kaever, A. Gründling, *PLoS Path.* **2011**, *7*, e1002217; b) B. W. Davies, R. W. Bogard, T. S. Young, J. J. Mekalanos, *Cell* **2012**, *149*, 358–370; c) P. Ross, H. Weinhouse, Y. Aloni, D. Michaeli, P. Weinberger-Ohana, R. Mayer, S. Braun, E. de V-room, G. A. van der Marel, J. H. van Boom, M. Benziman, *Nature* **1987**, *325*, 279–281; d) G. Witte, S. Hartung, K. Büttner, K. P. Hopfner, *Mol. Cell* **2008**, *30*, 167–178.
[7] A. Decout, J. D. Katz, S. Venkatraman, A. Ablasser, *Nat. Rev. Immunol.* **2021**, *21*, 548–569.
[8] H. Ishikawa, G. N. Barber, *Nature* **2008**, *455*, 674.
[9] a) S. Liu, X. Cai, J. Wu, Q. Cong, X. Chen, T. Li, F. Du, J. Ren, Y.-T. Wu, N. V. Grishin, Z. J. Chen, *Science* **2015**, *347*, aaa2630; b) R. Fang, C. Wang, Q. Jiang, M. Lv, P. Gao, X. Yu, P. Mu, R. Zhang, S. Bi, J.-M. Feng, Z. Jiang, *J. Immunol.* **2017**, *199*, 3222.
[10] J. Wu, N. Dobbs, K. Yang, N. Yan, *Immunity* **2020**, *53*, 115–126.e115.
[11] a) M. F. Gulen, U. Koch, S. M. Haag, F. Schuler, L. Apetoh, A. Villunger, F. Radtke, A. Ablasser, *Nat. Commun.* **2017**, *8*, 427; b) J. Sarhan, B. C. Liu, H. I. Muendlein, C. G. Weindel, I. Smirnova, A. Y. Tang, V. Ilyukha, M. Sorokin, A. Buzdin, K. A. Fitzgerald, A. Poltorak, *Cell Death Differ.* **2019**, *26*, 332–347.
[12] L. Andreeva, B. Hiller, D. Kostrewa, C. Lässig, C. C. de Oliveira Mann, D. J. Drexler, A. Maiser, M. Gaidt, H. Leonhardt, V. Hornung, K.-P. Hopfner, *Nature* **2017**, *549*, 394.
[13] a) J. Zhou, Y. Zheng, B. T. Roembke, S. M. Robinson, C. Opoku-Temeng, D. A. Sayre, H. O. Sintim, *RSC Adv.* **2017**, *7*, 5421–5426; b) R. W. Sinkeldam, N. J. Greco, Y. Tor, *Chem. Rev.* **2010**, *110*, 2579–2619.
[14] D. Shin, R. W. Sinkeldam, Y. Tor, *J. Am. Chem. Soc.* **2011**, *133*, 14912–14915.
[15] B. Novotná, L. Vaneková, M. Zavřel, M. Buděšínský, M. Dejmek, M. Smola, O. Gutten, Z. A. Tehrani, M. Pimková Polidarová, A. Brázdová, R. Liboska, I. Štěpánek, Z. Vavřina, T. Jandušík, R. Nencka, L. Rulíšek, E. Bouřa, J. Brynda, O. Páv, G. Birkuš, *J. Med. Chem.* **2019**, *62*, 10676–10690.
[16] Y. Li, A. Fin, A. R. Rovira, Y. Su, A. B. Dippel, J. A. Valderrama, A. M. Riestra, V. Nizet, M. C. Hammond, Y. Tor, *ChemBioChem* **2020**, *21*, 2595–2598.
[17] S. M. Ching, W. J. Tan, K. L. Chua, Y. Lam, *Bioorg. Med. Chem.* **2010**, *18*, 6657–6665.
[18] X. Zhang, H. Shi, J. Wu, X. Zhang, L. Sun, C. Chen, Z. J. Chen, *Mol. Cell* **2013**, *51*, 226–235.
[19] A. Fuchs, P. Mannhardt, P. Hirschle, H. Wang, I. Zaytseva, Z. Ji, O. M. Yaghi, S. Wuttke, E. Ploetz, *Adv. Mater.* **2021**, *34*, 2104530.
[20] a) G. I. Redford, R. M. Clegg, *J. Fluoresc.* **2005**, *15*, 805; b) M. A. Digman, V. R. Caiolfa, M. Zamai, E. Gratton, *Biophys. J.* **2008**, *94*, L14-L16; c) G. Weber, *J. Phys. Chem.* **1981**, *85*, 949–953; d) D. M. Jameson, E. Gratton, R. D. Hall, *Appl. Spectrosc. Rev.* **1984**, *20*, 55–106.